Journal of Archaeological Science 162 (2024) 105922

Contents lists available at ScienceDirect

Journal of Archaeological Science

journal homepage: www.elsevier.com/locate/jas

Past rainfall patterns in Southeast Asia revealed by microanalysis of $\delta^{18}O$ values in human teeth

Petra Vaiglova [a,b,c,*], Janaína N. Ávila [b,d], Hallie Buckley [e], Jean Christophe Galipaud [f], Daniel R. Green [c,g], Siân Halcrow [e], Hannah F. James [h], Rebecca Kinaston [b,i], Marc Oxenham [a,j], Victor Paz [k], Truman Simanjuntak [l], Christophe Snoeck [h], Hiep Hoang Trinh [m], Ian S. Williams [n], Tanya M. Smith [b,c]

[a] School of Archaeology and Anthropology, The Australian National University, Australia
[b] Griffith Centre for Social and Cultural Research, Griffith University, Australia
[c] Australian Research Centre for Human Evolution, Griffith University, Australia
[d] School of Earth and Environmental Science, University of Queensland, Australia
[e] Department of Anatomy, University of Otago, New Zealand
[f] Research Institute for Development, National Museum of Natural History Paris, France
[g] Department of Human Evolutionary Biology, Harvard University, USA
[h] Archaeology, Environmental Changes & Geo-Chemistry Research Group, Vrije Universiteit Brussel, Belgium
[i] BioArch South, Waitati, New Zealand
[j] School of Archaeology, University of Aberdeen, UK
[k] Archaeology Studies Program, University of the Philippines, Philippines
[l] National Research and Development Centre for Archaeology, Indonesia
[m] Department of Prehistoric Archaeology, Vietnam Institute of Archaeology, Vietnam, UK
[n] Research School of Earth Sciences, Australian National University, Australia

ARTICLE INFO

Keywords:
Oxygen isotope values
Strontium isotope ratios
Tooth chemistry
Ion microprobe
Seasonality
Paleoenvironment

ABSTRACT

Variations in human subsistence and settlement patterns have been documented at Holocene archaeological sites across Island and Mainland Southeast Asia. Although climate is frequently invoked as a causal mechanism underlying this variation, direct evidence of ancient rainfall variability on the scale of human lifetimes has thus far been elusive. Here we use a novel time-resolute method for *in situ* measurement of human tooth enamel $\delta^{18}O$ values (n = 2629 near-weekly measurements sampling 51 years) to assess past rainfall seasonality patterns in Southeast Asia. Seasonal fluctuations in enamel $\delta^{18}O$ values of ancient humans from several different periods are compared to modern rainfall recorded in Vietnam, Philippines, and Indonesia by the Global Network in Isotopes in Precipitation (GNIP). The likelihood that the ancient humans reflect local precipitation patterns is established through measurement of bulk enamel $^{87}Sr/^{86}Sr$ ratios. Comparison of the archaeological individuals and the modern rainfall datasets shows that the seasonal variabilities in ancient $\delta^{18}O_{enamel}$ are consistent with seasonal variabilities in modern $\delta^{18}O_{precip}$ across the study locations (highest in Vietnam, lowest in Indonesia, intermediate in the Philippines). Strong seasonal $\delta^{18}O_{enamel}$ trends in four of five hunter-gatherers from Con Co Ngua, Vietnam, facilitate the inference of birth approximately six months prior to the onset of monsoons, consistent with tropical subsistence societies where food availability correlates with rainfall. High-resolution analysis of human tooth enamel represents a powerful new tool for seasonality reconstructions across different regional and climatic settings.

1. Introduction

Paleoclimate research in Southeast Asia has largely focused on reconstructing the timing and character of past ice ages (van der Kaars et al., 2000; Cheng et al., 2016; Wang et al., 2018), shifts in monsoonal activity (Cheng et al., 2016; Semah et al., 2004; Wang et al., 2008;

* Corresponding author. School of Archaeology and Anthropology, The Australian National University, 44 Linnaeus Way, Acton, 2601, Australia
E-mail address: petra.vaiglova@anu.edu.au (P. Vaiglova).

https://doi.org/10.1016/j.jas.2023.105922
Received 15 August 2023; Received in revised form 15 December 2023; Accepted 15 December 2023
Available online 28 December 2023

Stephens et al., 2008; Griffiths et al., 2009; Lewis et al., 2011; Marwick and Gagan, 2011; Cai et al., 2015; Konecky et al., 2016; Zhao et al., 2017), and changing vegetation histories (van der Kaars et al., 2000; Haberle, 1998; Wurster et al., 2010, 2017; Wicaksono et al., 2015, 2017; Hamilton et al., 2019). The results suggest that in the early Holocene, the climate became wetter and climatic variability declined. A warm Holocene Climate Optimum was reached around 8000–5000 years ago (8–5 ka) (Semah et al., 2004; Hamilton et al., 2019) and the East Asian Summer Monsoon brought a wet, warm, and subtropical climate, which weakened after 5.7 ka[12]. Griffiths et al. (2009) present speleothem records that indicate that the last 2500–3000 years appear fairly stable and similar to modern day conditions.

Bioarchaeological research on the Holocene of Southeast Asia has focused primarily on mobility and settlement patterns of Neolithic coastal societies, particularly around and after the 4.2 ka event that saw the aridification of a number of regions around the world (Park et al., 2019; The Routledge Handbook of Bioarchaeology, 2016). Scholars have also directed considerable effort to studying the spread of farming, using combined linguistic, genetic, and archaeological evidence to infer long-distance mobility of island dwelling communities and movement of their material goods (Reepmeyer et al., 2011; Huffer et al., 2016; Lloyd-Smith et al., 2016; Vallée et al., 2016; Higham, 2021; Pawlik, 2021). An influential model by Bellwood, 2005, 2011 posited that migrating farmers moved from modern-day Taiwan into the northern Philippines by 2000 BCE and subsequently westwards into Indonesia and southeastwards into the Bismark archipelago by 1350 BCE (Oxenham et al., 2016). Research that followed focused on tracing archaeological evidence to support or refute this model, but direct inferences of climatic patterns and changes that would have hindered or facilitated such movements are still lacking.

1.1. Rainfall regimes

Rainfall is a key climatic factor that shapes the structure of tropical ecosystems (Brockman and van Schaik, 2005; Schwartz et al., 2020). Understanding changing rainfall patterns is not only useful for tracking the impact of past and present climate variation, but also for understanding human adaptations to environments and cultural experiences. A common approach to describe rainfall regimes, Mean Annual Precipitation (MAP), provides only partial insight into the degree to which rainfall patterns differ across geographical areas. Rainfall seasonality indices (Walsh and Lawler, 1981; Feng et al., 2013) have been developed to assess relative seasonality (defined as a dimension of seasonality encompassing contrasts between seasons) across geographical regions, with higher indices characterizing areas where rainfall is more concentrated in a given month/season and lower indices describing regions with a more uniform distribution of rainfall. These indices have been found to be better correlated with functional traits and life histories of tropical organisms than MAP or the length of the dry season (Schwartz et al., 2020).

Similarly, stable oxygen isotope compositions of precipitation ($\delta^{18}O_{precip}$ values)—which are controlled by air temperature, rainfall amount, latitude, altitude, and movements of water masses—show different degrees of seasonal variability in different regions (Epstein and Sharp, 1959; Dansgaard, 1964; Sharp, 2017). In regions with pronounced seasonal $\delta^{18}O_{precip}$ variability, large contrasts exist between summer and winter $\delta^{18}O_{precip}$ values. In regions with 'dampened' seasonal $\delta^{18}O_{precip}$ variability, these differences are reduced. For example, in a continent-wide study of rainfall across Australia, seasonal $\delta^{18}O_{precip}$ variability as high as ~12 ‰ was identified at Mount Isa in the central inland region, while dampened seasonal $\delta^{18}O_{precip}$ variability of ~2 ‰ was identified at Perth on the west coast (Hollins et al., 2018). In the tropics, rainfall amount is the primary determinant of rainfall stable isotope composition (Dansgaard, 1964; Gat, 1996; Bowen, 2010).

1.2. Assessment of ancient climate and seasonality

To understand the impact of shifting climate on the sub-annual scale, a range of methodologies has been used to extract seasonality patterns from trees, corals, ocean sediments, and speleothems. Poussart et al. (2004) measured the $\delta^{18}O$ values of cellulose from seasonal tree-rings and extracted a record of distinct seasonal variability in $\delta^{18}O_{precip}$ values across Southeast Asia (18 ‰ in Thailand and 4 ‰ in Indonesia). Yang et al. (2016) assessed the factors that drive inter-annual variability in $\delta^{18}O$ values of speleothems at four cave sites affected by the Asian monsoon (Oman, India, Laos, China). These authors argued that while precipitation amounts might correlate with annual seasonal patterns in rainfall, they cannot be used to document multi-annual phenomena, such as the El Niño-Southern Oscillation (ENSO).

Stable oxygen isotope measurements of tooth enamel ($\delta^{18}O_{enamel}$), which reflect the composition of water, food, and air consumed by the individual during tooth formation (Bryant and Froelich, 1995; Kohn, 1996), provide a means to infer aspects of past climatic conditions. Despite the contribution of food and air to metabolically produced water and hard tissue $\delta^{18}O$ values, foundational studies in oxygen isotope systematics have shown a strong relationship between bioapatite (the mineral component of tooth enamel) and local meteoric water oxygen isotope compositions (Kohn, 1996; Longinelli, 1984; Green et al., 2022; Longinelli and Peretti Padalino, 1983; d'Angela and Longinelli, 1990). For example, (Green et al., 2022 established an association between local monthly rainfall amounts in Ethiopia, $\delta^{18}O$ measurements from an upstream water source, and $\delta^{18}O_{enamel}$ values from modern baboon (*P. hamadryas*) tooth enamel formed concurrently. Moreover, their comparisons of $\delta^{18}O_{enamel}$ values between sympatric Ugandan primate species with different diets revealed highly overlapping ranges with relatively minor average differences (~1 ‰).

The majority of previous studies in paleoecology have applied either a 'bulk' or a macroscopic 'sequential' sampling method for extracting $\delta^{18}O_{enamel}$ values (Pederzani and Britton, 2019; Vaiglova et al., 2022). Bulk sampling involves the extraction of one homogenized sample per individual, often drilled along the entire length of the preserved tooth. For example, King et al. (2013) analyzed bulk enamel samples from 118 human burials at Ban Non Wat (Thailand) spanning the Neolithic (1750 BCE) through to the Iron Age (400 AD), and reported evidence for a shift from lower to higher aridity that may have negatively impacted rice cultivation. Macroscopic sequential sampling uses enamel samples drilled along the axis of tooth development to assess isotopic changes in diet and water intake during the period of tooth formation. Kubat et al. (2023) reported three $\delta^{18}O_{enamel}$ values obtained from an Indonesian *Homo erectus* premolar, suggesting that it obtained water from a largely invariant riverine water source. However, because such macroscopic samples cut across incrementally forming enamel, their $\delta^{18}O_{enamel}$ values provide an averaged, and dampened, record of the isotopic composition of the individual's body water and associated food and drinking water. Thus, these samples need to be considered as arbitrary units homogenizing a loosely known amount of isotopic input signal (Balasse, 2003). Nevertheless, sequential isotopic data extracted from teeth have the potential to inform us about broad-scale climate patterns in the past in order to understand people's experiences of, and adaptation to, their local environments.

Secondary ion mass spectrometry (SIMS) enables measurement of the innermost enamel *in situ* at a scale of a few microns. Blumenthal et al. (2014) first demonstrated the use of this technique through measurement of modern tooth enamel of captive woodrats. Most recently, a Sensitive High-Resolution Ion Microprobe (SHRIMP) was used to analyze histological sections of hominin and primate teeth, enabling successive measurements of $\delta^{18}O_{enamel}$ at a spatial resolution equivalent to approximately one week of enamel extension (Green et al., 2022; Smith et al., 2018). For example, Smith et al. (2018) used this technique to compare climate seasonality recorded in the teeth of two Neanderthals (~250 ka) and one Holocene individual (5 ka) from Payre, France.

They argued that the studied Neanderthals experienced a cooler and more seasonal climate compared to the Holocene individual from the same location; consistent with climate reconstructions obtained from speleothem records in southern France, northern Italy, and southern Ireland (McDermott et al., 1999). Similarly, Smith et al. (2023) measured $\delta^{18}O_{enamel}$ values in orangutans from the islands of Borneo and Sumatra, finding annual and bimodal trends in recent Sumatra individuals that are consistent with modern rainfall data. Comparisons of recent Bornean orangutans with two late Pleistocene/early Holocene individuals from Niah Cave suggest drier and more open environments with reduced monsoon intensity during this earlier period, consistent with other Niah Caves studies and long-term speleothem $\delta^{18}O$ records in the broader region.

Here we apply the SHRIMP (SIMS) method to extract sequential $\delta^{18}O_{enamel}$ values from 15 ancient human teeth recovered at three archaeological sites in Southeast Asia: Con Co Ngua (CCN), Vietnam, ~6800–6200 cal BP; Pain Haka (PH), Indonesia, ~3000–2100 cal BP; Napa (NP), Philippines, ~2000–1500 cal BP (Fig. 1). Bulk strontium isotope ratios ($^{87}Sr/^{86}Sr$) (one per archaeological tooth), commonly used to identify non-local individuals by comparison to local bedrock $^{87}Sr/^{86}Sr$ ratios (Bentley, 2006), are used to assess the likelihood that the studied individuals were born away from the location where they were buried and thus record non-local rainfall. Data obtained from the Global Network of Isotopes in Precipitation (GNIP) database are used to assess the seasonal variability of $\delta^{18}O_{precip}$ values measured near the study locations in the 20th–21st century. The recorded seasonality in the archaeological teeth is compared with the expected patterns of seasonal variability of modern $\delta^{18}O_{precip}$ at the study locations. In addition, two modern human teeth from Australasia (Southeastern Queensland, Australia; Dunedin, New Zealand: Fig. 1) are used to investigate the suitability of postindustrial human teeth for inferring seasonal rainfall patterns.

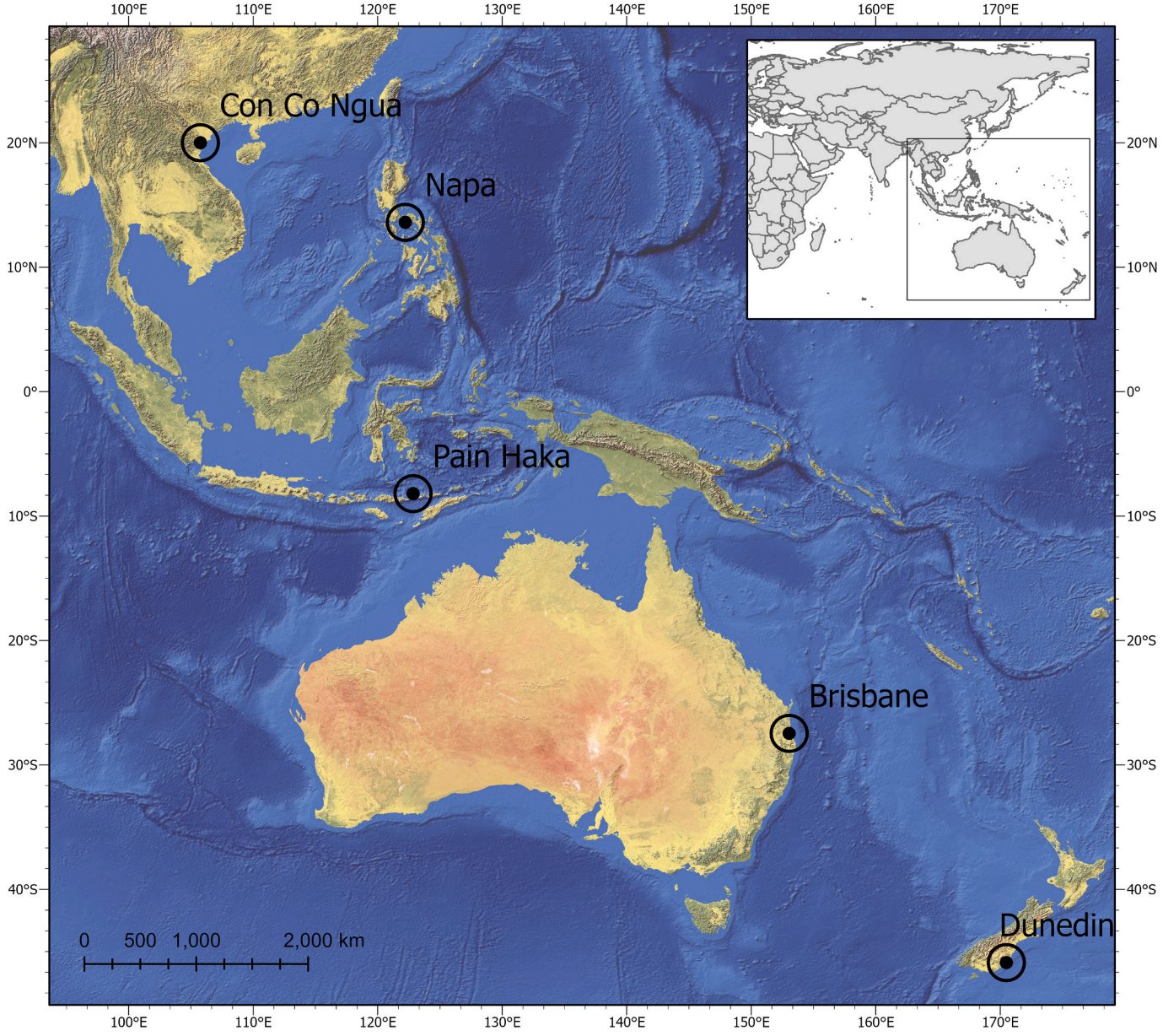

Fig. 1. Map of Southeast Asia showing locations of archaeological sites and GNIP stations. Created using ArcGIS Pro v 2.9.5 and basemap, 1:10 m Natural Earth I with Shaded Relief and Water, provided permission free by Natural Earth.

2. Materials and methods

2.1. Archaeological and modern samples

The archaeological sites in this study represent coastal settlements and burial grounds that were in use across Southeast Asia over a period of ~5000 years. Con Co Ngua, Vietnam, is a large open-air hunter-gatherer site dating to the Da But cultural complex, which stretched across Northern Vietnam and Southern China between ~6800 and 6200 cal BCE (Oxenham et al., 2018). The inhabitants continued to maintain a foraging subsistence strategy during a time when farmers further to the north (in Southern China) were becoming more and more reliant on agriculture; thus representing an alternative adaptation to the Holocene Climate Optimum (Oxenham et al., 2018). The five individuals included here (all first molars, M1s) represent individuals recovered from burials from Layer 2 (older) and Layer 1 (younger) (Huffer et al., 2016).

Pain Haka, Indonesia, is located on the island of Flores and represents a coastal cemetery, stretching over 700 m along the shoreline, that seems to have been most heavily used around 2500 BP[59,60]. No occupation layers have been uncovered at the site, raising speculation that the cemetery may have been used to inter people from across wider reaches of the island region. All five individuals included in this study were represented by M1s. Four individuals (PH10, PH22, PH45, PH47B) were directly dated in this study using AMS radiocarbon dates to 3004–2363 cal BP (see Table S2).

Napa (Location 1), originally referred to as Catanauan, Philippines, represents a collection of two coastal cemeteries situated on a beach within a sheltered cove on the western part of the Bondoc peninsula, Philippines. The main cemetery dates to the first half of the first millennium AD (Metal Period) and was probably used for a period of 100–200 years, a period characterized by distinct pottery and burial grave goods including metal objects (short swords/daggers, iron blades/knives), beads (made of shell, glass, carnelian), and other shell objects (both worked and unworked). A large number of human remains has been uncovered from varying depositional contexts, including jar burials, extended burials, and pit burials (Paz et al., 2018). Four individuals from Napa, Philippines (1 M1, 1 M2, 2 M3s) date to the Metal Period (~2000–1500 cal BP) (Vlok et al., 2017) and one individual (C507A; M2), recovered ~100 m from the site, represents a more recent (although not modern) individual.

Two living human M1s were also examined: one from the east coast of Australia (Southeastern Queensland, T1) born in 1990 and one from the South Island of New Zealand (MS5) born in 2011. See Table S2 for contextual information.

2.2. Modern rainfall data

Modern (20th–21st century) rainfall data were obtained from the Global Network of Isotopes in Precipitation (GNIP, International Atomic Energy Agency (Global, 2022)). In Vietnam, the closest stations to Con Co Ngua (20° 0′ 16.53″ N, 105° 45′ 33.85″ E) are Hanoi (21° 20′ 43.24″ N, 105° 47′ 55.20″ E; $\delta^{18}O$ values of precipitation measured between 2004 and 2007) and Hanoi IGS (21° 1′ 48″ N, 105° 50′ 24″ E; $\delta^{18}O$ values of precipitation measured between 2015 and 2018). In Indonesia, the closest GNIP station to Pain Haka (8° 11′ 35.36″ S, 122° 50′ 23.53″ E) is Jakarta (6° 10′ 47.99″ S, 106° 49′ 48″ E; 1962–1997). Belgamann et al. (Belgaman et al., 2017) obtained rainfall $\delta^{18}O$ values from locations closer to Pain Haka that cover a period of 3 years (2010–2012), however, because these locations were identified to fall into the same cluster as Jakarta (according to the variability in seasonal $\delta^{18}O_{precip}$ values) and because the GNIP database provides a longer temporal coverage, the GNIP data are used in this study as a comparative dataset. In the Philippines, the closest stations to Napa (13° 36′ 29.88″ N, 122° 12′ 54.93″ E) are Manila (14° 31′ 11.99″ N, 121° 0′ 0″ E; 1961–1976) and Diliman Quezon (14° 38′ 24″ N, 121° 2′ 24″ E; 2000–2016). In Australia, T1 grew up near the station in Brisbane (27° 25′ 47.99″ S; 153° 4’ 48” E). GNIP data was not available for New Zealand, but the Waterisotopes Database (http://waterisotopesDB.org, accessed November 2022) provided $\delta^{18}O$ values of precipitation measured at the location Dunedin City (2007–2009; Project ID: 00204) (Frew et al., 2011).

2.3. High-resolution sequential tooth $\delta^{18}O$ analyses

The tooth enamel $\delta^{18}O$ values were measured by ion microprobe (SHRIMP–SI) at the Australian National University, as detailed in Smith et al. (2018). In brief, tooth enamel in thin sections was first imaged with transmitted light microscopy, accentuated growth lines were mapped, daily secretion rates were measured, and enamel extension rates were calculated to guide spot placement at approximately weekly intervals of growth from the dentine horn tip to the enamel cervix. Following the removal of cover slips with xylene, the sections were cleaned with petroleum spirit, warm RBS35 detergent solution and millipore water, dried for at least 24 h in a 60 °C vacuum oven, coated with ~10 nm of high purity Al, mounted in a sample holder, and placed in the SHRIMP vacuum lock for at least 12 h to outgas.

A 15 kV Cs^+ primary ion beam of ~2 nA focused to a spot ~15 × 20 μm diameter was used to sample the enamel sequentially as close as possible (≤30 μm) to the enamel-dentine junction (EDJ). Negative O secondary ions were extracted at 10 kV. Mass resolution was approximately 1800 and 2400 for $^{16}O^-$ and $^{18}O^-$ (m/Δm, 10% peak height), respectively. The low mass head and high mass head detectors, equipped with Faraday cups, were used for the simultaneous detection of $^{16}O^-$ and $^{18}O^-$, respectively. The electrometers measuring $^{16}O^-$ and $^{18}O^-$ were set to 10^{11} Ω (50 V range) and 10^{11} Ω (5 V range), respectively, mass analyzed at ~ 3000 R, and $^{18}O/^{16}O$ measured by multiple collector using resistor-mode electrometers (^{16}O 10^{11} Ω, ^{18}O 10^{12} Ω). Charging of the tooth surface was neutralized using a broadly focused ~1.2 kV electron beam. Each analysis consisted of ~2 min preconditioning, during which electrometer baselines were measured, followed by ~1 min optimization of the beam steering and 6 × 20 s measurements of $^{18}O/^{16}O$. Corrections were made for electron-induced secondary ion emission (EISIE, Ickert et al., 2008) measured before and after each analysis. The $\delta^{18}O$ values were calculated relative to analyses of reference apatite Durango 3 ($\delta^{18}O_{SMOW}$ = 9.8‰; Rigo et al., 2012) spaced every 10–15 sample analyses throughout the analytical session. Count rates of ~0.6–1.0 GHz for ^{16}O yielded a single spot $\delta^{18}O$ uncertainty of ~0.1‰ (1 SD) and repeatability on the reference material of commonly 0.4–0.5‰ (2 σ). All $\delta^{18}O$ values are reported relative to the VSMOW scale.

Distances of SHRIMP $\delta^{18}O$ measurements along the innermost enamel from the cusp to cervix of each tooth were converted to time in days using incremental features of growth observed in the teeth through transmitted light microscopy. This was accomplished through two steps. First, the timing of enamel extension at the innermost enamel was determined at each of a series of accentuated lines, such that the distance of any given accentuated line at its intersection with the EDJ was associated with a day of extension relative to the onset of enamel formation in that cusp. Second, a polynomial regression relating distances to days was created using the distance-day measurements from accentuated lines at the enamel-dentine junction, and this regression was applied to calculate the timing of secretory deposition at every SHRIMP spot location.

To estimate the season of birth, we hypothesized seasonal climatic variation that results in annual oscillations in oxygen isotope values within teeth. We further predicted that these oscillations have a sinusoidal form, that their amplitudes of variation are equal to the range of variation observed in each M1, but that the offset of the sine wave (that is, the day the tooth begins forming in the seasonal cycle) is unknown. We defined the middle of the monsoon and the middle of the dry season isotopically, as the lowest and highest points in the sinusoidal curve, following known patterns of isotopic and climatic variability in the region. Then, we selected a seasonal offset for our hypothetical sine curve

that best matched observations using the curve fit function in Python's SciPy package, using a least-squares metric of fit. This procedure describes when a tooth most likely began forming over multiple seasons, which was then related to the neonatal (birth line) and added to prenatal formation time (i.e., relating the predicted seasonal patterns to the day of birth.) This approach was applied to the four Vietnamese individuals that showed the strongest annual isotopic patterns over multiple years.

2.4. $^{87}Sr/^{86}Sr$ ratio analyses

$^{87}Sr/^{86}Sr$ ratios of the ancient individuals were used to determine whether any of them were non-local to the site where they were buried (and thus recording non-local seasonality signals). Samples from Napa and Con Co Ngua were analyzed at the Vrije Universiteit Brussel (VUB), Belgium. Tooth enamel was drilled from the cusp of the tooth avoiding regions identified as containing diagenetic overprint. This resulted in sampling of a latitudinal transect of surface enamel extending from the occlusal surface down to up to three-quarters distance to the cervix. The tooth enamel powder was pre-treated with 0.1 M acetic acid (CH_3COOH) solution in excess for 30 min followed by three milliQ^{TM} water rinses and dried overnight at 50 °C (Pellegrini and Snoeck, 2016). 10 mg of sample was then acid digested in 1 mL 14 M nitric acid overnight and evaporated to dryness, before strontium was extracted through column chemistry using ion exchange resin (Eichrom Sr Spec). In short, the columns and resin were rinsed 2 × with 2 M HNO_3 then 2 × 7 M HNO_3, samples loaded in 7 M HNO_3, charged 4 × 1 mL 7 M HNO_3, and columns were eluted and Sr collected with 6 × 1 mL 0.05 M HNO_3. Samples were measured on a Nu Plasma 3 MC-ICP Mass Spectrometer (PD017 from Nu Instruments, Wrexham, UK) at the Vrije Universiteit Brussel. During the course of this study, repeated measurements of the NBS987 standard yielded $^{87}Sr/^{86}Sr = 0.710240 \pm 24$ (2σ for 60 analyses), which is, for our purposes, sufficiently consistent with the mean value of 0.710252 ± 13 (2σ for 88 analyses) obtained by TIMS (Thermal Ionization Mass Spectrometry) instrumentation (Weis et al., 2006). Data were corrected for mass fractionation by internal normalization to $^{86}Sr/^{88}Sr = 0.1194$. All the sample measurements were normalized using a standard bracketing method with the recommended value of $^{87}Sr/^{86}Sr = 0.710248$ (Weis et al., 2006). Procedural blanks were considered negligible (total Sr (V) of max 0.02 versus 9–10 V for analyses; i.e. ≈ 0.2%). For each sample the $^{87}Sr/^{86}Sr$ ratio is reported with a 2σ error.

Strontium concentrations were measured on the five tooth enamel samples from Napa. Samples were pre-treated as above and digested in Teflon beakers (Savillex) using subboiled 14 M HNO_3 at 120 °C for 24 h, evaporated to near-dryness and subsequently digested with a drop of concentrated HNO_3. Following dilution with 2% HNO_3, Sr and Ca concentrations in the sample digests were determined using a ATTOM ES HR-ICP mass spectrometer from Nu Instruments at the Vrije Universiteit Brussel (VUB), Belgium, in low (^{88}Sr) and medium (^{44}Ca) resolution using Indium (In) as an internal standard and external calibration versus various reference materials (SRM1400, SRM1486, SRM1515). The actual strontium concentrations were then calculated by normalizing the calcium data to 40% wt. Accuracy was evaluated by the analysis of an internal bioapatite standard (CBA). Based on repeated digestion and measurement of these reference materials, the analytical precision of the procedure outlined above is estimated to be better than 5% (1σ, n = 10 for CBA).

Samples from Pain Haka were analyzed at the Max Planck Institute for Evolutionary Biology (MPI) as part the analysis of the entire Pain Haka skeletal assemblage. To remove possible surface contaminants, the tooth surfaces were abraded using a sonicated Dremel® rotary tool with a diamond tipped burr. Then, using a Dremel® diamond cutting wheel, a 10–20 mg sample of enamel was removed from the tooth and adhering particles, such as organic matter or dentine, were also removed. The enamel samples were weighed, then 2 mL of 65% HNO_3 was pipetted into a Savillex beaker. The beakers were capped and the samples were digested for 2 h at a temperature of 120 °C on a hot plate. Once fully digested, lids were removed from the beakers and the samples were dried for 8 h at 120 °C. After evaporation, samples were dissolved in 1 mL of 3 M HNO_3. Each batch contained a blank and a standard (NIST SRM 1486, bone meal) to act as controls during the sample preparation. Strontium was purified using established processes of column chemistry (Deniel and Pin, 2001) fully described in Kramer et al. (2021). After the purification was complete, samples were dissolved in 3% HNO_3 and analyzed using a Thermo Fisher Neptune MC-ICP-MS instrument. $^{87}Sr/^{86}Sr$ ratios were normalized using repeated measurements of the NIST-SRM 987 standard. The five bone meal standards (SRM 1486) gave consistent results with the expected value: average $^{87}Sr/^{86}Sr = 0.70929 \pm 0.00002$ for five runs total (long term value measured at this lab: 0.709300 ± 0.000026 1σ, n = 88).

2.5. Radiocarbon dating

Four individuals from Pain Haka included in this study (PH10, PH22, PH45, PH47B) were radiocarbon dated using Accelerator Mass Spectrometry (AMS) at the Radiocarbon Dating Laboratory, University of Waikato. Collagen was extracted from bone samples using a modified Longin (1971) protocol. Samples were demineralized in 1 M HCl for up to 4 days, rinsed in MilliQ™ water, and gelatinized by heating in weakly acidic water (pH3 at 90 °C for 4 h). They were subsequently ultrafiltered (using pre-cleaned Centriprep®, Ultracel YM-30 filters) and freeze-dried (using a Labconco FreeZone Triad freeze-dryer backed by an Edwards nXDS10i series oil-free pump) for a minimum of 48 h before being turned into graphite for AMS dating.

3. Results

3.1. Sequential tooth enamel $\delta^{18}O$ values and modern rainfall

The measured tooth enamel $\delta^{18}O$ values ($\delta^{18}O_{enamel}$) range from +11.6 to +19.8 ‰ for individuals from Vietnam, +13.8 to +20.9 ‰ for individuals from the Philippines, +14.8 to +21.0 ‰ for individuals from Indonesia, +18.7 to +21.6 ‰ for the modern individual from New Zealand, and +17.8 to +21.5 for the modern individual from Australia (Table 1; all sequences are shown in Supplementary File S1). The individual intra-tooth amplitudes ($\Delta^{18}O_{tooth} = \delta^{18}O_{max} - \delta^{18}O_{min}$) range between 4.5 and 6.6 ‰ (Vietnam), 3.0 and 5.9 ‰ (Philippines), and 3.6 and 5.9 ‰ (Indonesia). The modern individuals record $\Delta^{18}O_{tooth}$ values of 2.9 ‰ (New Zealand), and 3.7 ‰ (Australia).

To assess annual seasonal variability, the sequences were broken down into year 1 (day 1–365), year 2 (day 366–731) and year 3 (day 732–1096) of tooth formation, and the remaining measurements discarded. The annual variability in $\delta^{18}O_{enamel}$ values for each year represented in the dataset is expressed as $\Delta^{18}O_{year}$ (Fig. 2). A full 3rd year was recorded in 11/15 archaeological samples and in the modern samples from Australia and New Zealand. In the modern sample from New Zealand, the year 1 portion of enamel was affected by a carious lesion, so only measurements for years 2 and 3 are considered. The $\Delta^{18}O_{year}$ values range between 3.3–6.0 ‰ (Vietnam), 2.1–4.4 ‰ (Philippines), 2.0–4.1 ‰ (Indonesia), 1.9–3.7 ‰ (Australia), and 1.5–2.2 ‰ (New Zealand) (Table 1).

Monthly $\delta^{18}O$ values of modern precipitation ($\delta^{18}O_{precip}$) measured at the station closest to the study site in Vietnam (Hanoi, 2004–2018; GNIP database) show pronounced differences between maximum (April) and minimum (August) $\delta^{18}O$ values. This highly seasonal trend correlates most closely with the trend in amounts of monthly rainfall, exhibiting an inverse correlation between the amount of rainfall and $\delta^{18}O_{precip}$ values (Dansgaard, 1964) (Fig. 3a and b). At the closest stations in the Philippines (Manila and Diliman Quezon, 1961–2016), the seasonal variability in $\delta^{18}O_{precip}$ was less pronounced than in Hanoi, but maximum values were detected in January–April and minimum values were detected in July–September. This trend also correlates most closely

Table 1
Summary statistics of $\delta^{18}O_{enamel}$ values and $^{87}Sr/^{86}Sr$ ratios of archaeological individuals from Con Co Ngua (Vietnam), Pain Haka (Indonesia), Philippines (Napa), and modern individuals from Australia (Southeastern Queensland) and New Zealand (Dunedin) measured in this study. VUB = Vrije Universiteit Brussel, Belgium; MPI = Max Planck Institute, Leipzig, Germany.

ID	Location	$\delta^{18}O_{min}$	$\delta^{18}O_{max}$	$\Delta^{18}O_{mean}$	$\Delta^{18}O_{year1}$	$\Delta^{18}O_{year2}$	$\Delta^{18}O_{year3}$	$^{87}Sr/^{86}Sr$	$^{87}Sr/^{86}Sr$ analyzed at
M26	Con Co Ngua, Vietnam	13.2	19.8	6.6	6.0	4.9	4.1	0.709358 ± 0.000007	VUB
M80	Con Co Ngua, Vietnam	12.4	17.8	5.4	3.7	3.9		0.709070 ± 0.000008	VUB
M101	Con Co Ngua, Vietnam	13.3	17.8	4.5	3.3	3.5	4.4	0.709434 ± 0.000009	VUB
M144	Con Co Ngua, Vietnam	12.4	18.6	6.2	4.6	3.9	4.9	0.709527 ± 0.000008	VUB
M145	Con Co Ngua, Vietnam	11.6	17.8	6.2	6.0	5.8	3.6	0.709573 ± 0.000008	VUB
C202	Napa, Philippines	15.5	19.8	4.3	2.1	3.5		0.708613 ± 0.000010	VUB
C403	Napa, Philippines	15.0	20.9	5.9	4.4	2.7	4.1	0.706584 ± 0.000008	VUB
C459	Napa, Philippines	13.8	18.2	4.4	3.1	2.1		0.705204 ± 0.000008	VUB
C507A	Napa, Philippines	15.1	19.7	4.6	3.7	3.8	2.8	0.707245 ± 0.000008	VUB
C552	Napa, Philippines	15.9	18.9	3.0	2.5	2.2	2.2	0.708064 ± 0.000008	VUB
PH10	Pain Haka, Indonesia	17.2	20.8	3.6	2.7	2.4	2.0	0.7077	MPI
PH22	Pain Haka, Indonesia	14.8	20.7	5.9	4.1	3.2	4.1	0.7074	MPI
PH34	Pain Haka, Indonesia	15.3	19.4	4.1	2.3	3.7	2.3	0.7076	MPI
PH45	Pain Haka, Indonesia	16.6	21.0	4.4	4.0	3.1		0.7075	MPI
PH47B	Pain Haka, Indonesia	16.0	20.1	4.1	2.2	3.0	3.7	0.7063	MPI
MS5	Dunedin New Zealand	18.7	21.6	2.9		2.2	1.5		
T1	Southeastern Queensland, Australia	17.8	21.5	3.7	3.7	1.9	2.3		

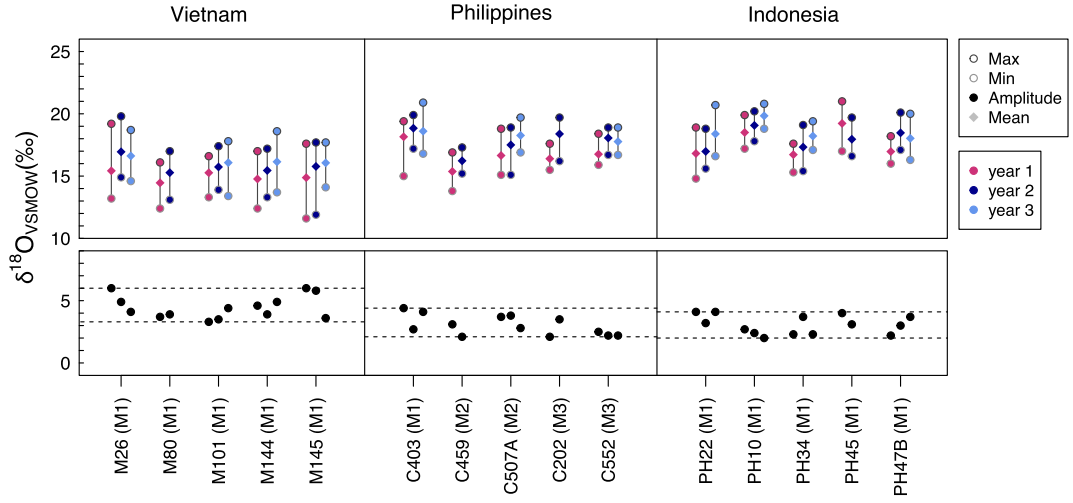

Fig. 2. Annual variability in $\delta^{18}O_{enamel}$ values for individual years represented in the archaeological dataset. The individual sequences were truncated into year 1 (day 1–365), year 2 (day 366–731) and year 3 (day 732–1096) of tooth formation and the measured values are summarized as maximum, minimum and mean $\delta^{18}O_{enamel}$ values for each year. On the bottom, the amplitudes of intra-tooth variation ($\delta^{18}O_{max} - \delta^{18}O_{min}$) are shown individually, and their range per geographical location is indicated with dashed lines.

(and inversely) with monthly amounts of precipitation (Fig. 3c and d). In Indonesia (Jakarta, 1962–1997) seasonal variability was even less pronounced, nevertheless showing slightly higher $\delta^{18}O_{precip}$ values between July–September (also see Belgaman et al., 2017). This lack of pronounced seasonality is most consistent with the rather flat trends in air temperature (Fig. 3f).

To better characterize annual seasonality in modern precipitation, the annual variability in $\delta^{18}O_{precip}$ values was calculated for each year represented in the modern dataset (Table S1). Only years where at least 9 monthly measurements were made were included. The rainfall in Vietnam showed the highest amplitude of seasonal variation ($\Delta^{18}O_{precip}$ = 10.7 ± 2.0 ‰, 1σ; over 7 years), followed by the Philippines ($\Delta^{18}O_{precip}$ = 8.2 ± 1.2 ‰, 1σ; over 21 years) and Indonesia ($\Delta^{18}O_{precip}$ = 5.9 ± 1.5 ‰, 1σ; over 15 years).

Considering the modern individuals, the closest GNIP station to where T1 spent their childhood is in Brisbane (Australia, 1970–2014). Although the decadal trends there do not show strong seasonality in the 1970s, 1980s, 2000s, and 2010s (Fig. S1), in the first two years of T1's life (1990–1991), the maximum and minimum $\delta^{18}O_{precip}$ values differed by 5.7 ‰ and 9.2 ‰, respectively (Table S1). Contrary to the pattern in the $\delta^{18}O_{precip}$ values, however, the amplitude of seasonal variation recorded in T1's first molar was smaller in year 2 (1991, 1.9 ‰) compared to year 1 (1990, 3.7 ‰; Table 1), likely a result of drinking attenuated tap water drawn from municipal reservoirs. In Dunedin, where MS5 spent their childhood and also drank tap water from rain tanks and municipal sources, $\delta^{18}O_{precip}$ data were available only between 2007 and 2009, prior to when MS5 was born (2011). The available data do not show strong seasonality in $\delta^{18}O_{precip}$ values (Fig. S1), explained by the predominantly marine climate (Yang et al., 2020). River $\delta^{18}O$ values have also been found to exhibit dampened seasonality on the South Island (where Dunedin is located) due to the blurring of composition as a result of the large contribution of snowmelt to rivers (Yang et al., 2020). Correspondingly, the annual seasonality recorded in the second and third year of MS5's life was equally low (2012: 2.2 ‰; 2013: 1.5 ‰; Table 1).

3.2. Tooth enamel $^{87}Sr/^{86}Sr$ ratios

Strontium isotope ratios were measured for all archaeological samples (one sample per individual) and show the greatest variation in the Philippines (0.7052–0.7086), and lowest variation in Vietnam (0.7091–0.7096) (Fig. 4). One sample from Indonesia (PH47B) displays

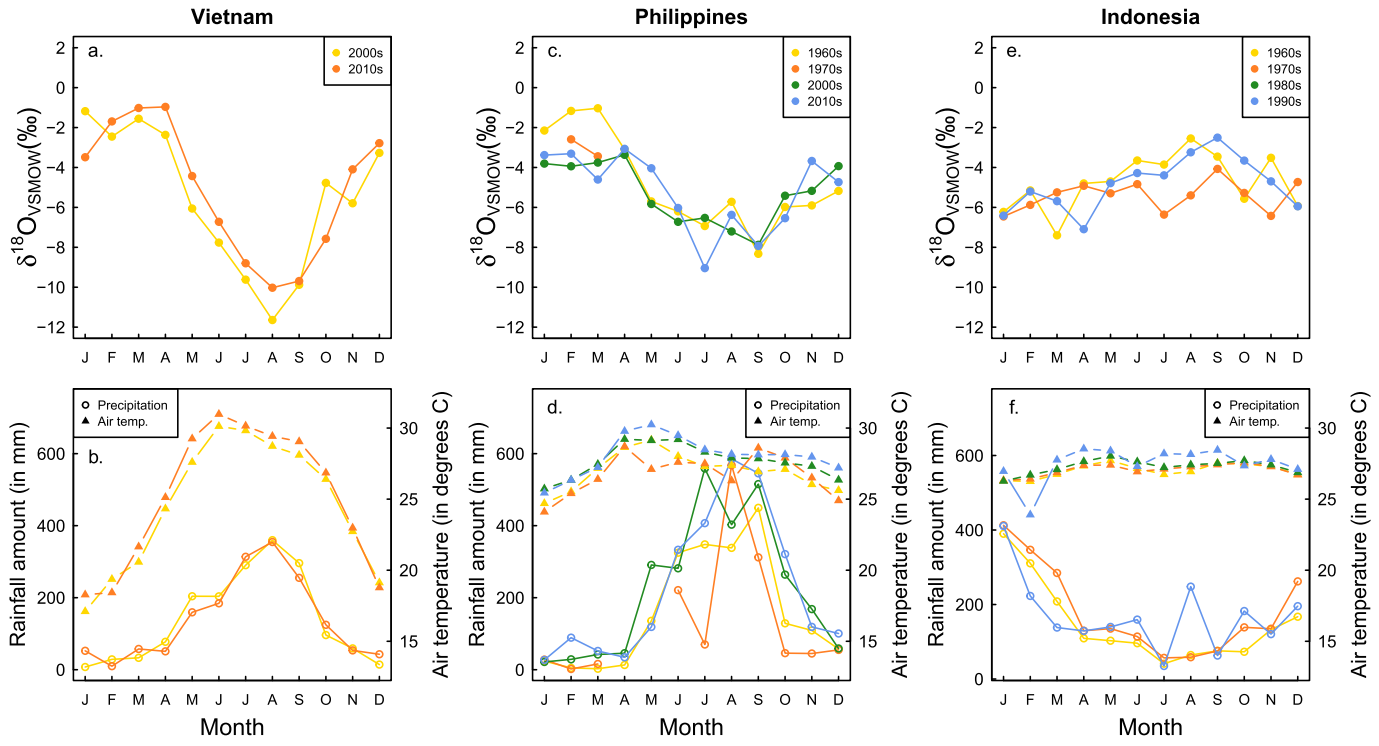

Fig. 3. Climate data obtained from the GNIP database summarizing rainfall collected at stations located closest to the archaeological sites (Vietnam: Hanoi; Philippines: Manila; Indonesia: Jakarta). The top panels show the annual variability in $\delta^{18}O_{precip}$ values and the bottom panels show trends in precipitation amounts and air temperature.

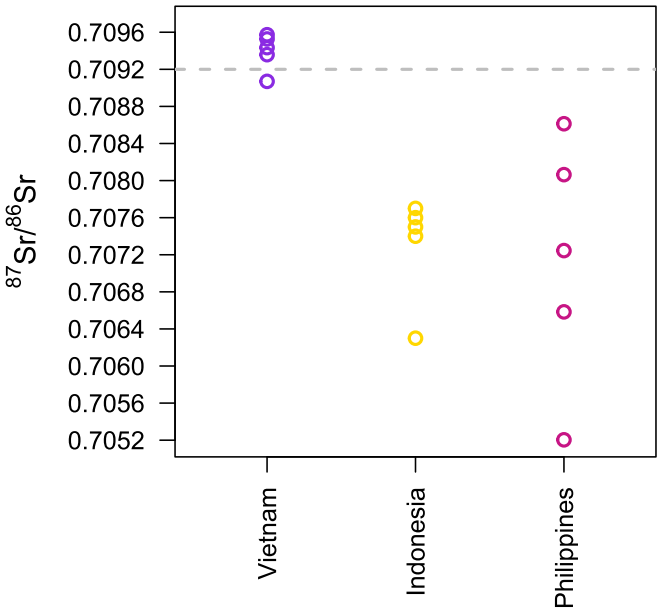

Fig. 4. $^{87}Sr/^{86}Sr$ ratios measured from the archaeological individuals from Con Co Ngua (Vietnam), Pain Haka (Indonesia), and Napa (Philippines). The dashed line indicates the $^{87}Sr/^{86}Sr$ value of seawater (McArthur et al., 2001).

a $^{87}Sr/^{86}Sr$ ratio 0.0012 lower compared to the average of the remaining four samples (averaging 0.7076 ± 0.0001). One sample from Vietnam (M80) has a $^{87}Sr/^{86}Sr$ ratio 0.0004 lower compared to the average of the remaining four samples (averaging 0.7095 ± 0.0001). The samples from Indonesia (0.7073 ± 0.0006, 1σ) fit within the larger range of $^{87}Sr/^{86}Sr$ ratios of the samples from the Philippines (0.7071 ± 0.0013; 1σ), with both groups displaying values well below the $^{87}Sr/^{86}Sr$ ratio of modern seawater (0.7092, McArthur et al., 2001). The samples from Vietnam fall into a higher range of ratios (0.7094 ± 0.0002, 1σ), which includes modern seawater.

4. Discussion

4.1. Tooth enamel, precipitation, and seasonality

Comparison of the archaeological individuals and the modern rainfall datasets shows that the seasonal variabilities in archaeological $\delta^{18}O_{enamel}$ resemble the seasonal variabilities in modern $\delta^{18}O_{precip}$ across the distinct latitudes (highest in Vietnam, lowest in Indonesia, intermediate in the Philippines). It is possible to estimate the season of birth from first molars of individuals from highly seasonal environments, as was done for a Neanderthal individual from Payre, France from its annually variable SHRIMP measurements (Smith et al., 2018). Four of five Vietnamese individuals were born six months prior to the peak of the monsoon (range ~155–225 days), consistent with reports of human birth seasonality in tropical subsistence societies where food availability correlates with rainfall (Bronson, 1995). Rainfall patterns in central Vietnam are driven by the shift in moisture source from the Indian Ocean (summer) to the South China Sea (winter), while most rainfall precipitates during the autumn season (Wolf et al., 2020). Modern rainfall patterns in Indonesia are controlled by the Asian monsoon (in the wet season) and the Australian monsoon (in the dry season) (Belgaman et al., 2017). A large proportion of rainfall in the Philippines is induced by tropical cyclones, with the highest contribution in the northern part of the country, attributed to the enhancement of the Asian monsoon (Bagtasa, 2017).

In the modern human teeth from Southeastern Australia and the South Island of New Zealand, the recorded patterns are largely flattened, exhibiting smaller annual amplitudes in $\delta^{18}O_{enamel}$ values (1.9–3.7 ‰, and 1.5–2.2 ‰, respectively; Table 1). This is consistent with the fact that the overall water intake of these individuals came from a range of sources not restricted to local rainfall, including city dams/reservoirs, rivers, large water tanks, and processed, boiled, or bottled water. While

showing that these data are sensitive enough to pick out these modern behaviors, the findings highlight that inferring the causal mechanisms of body/ingested water $\delta^{18}O$ values of contemporary individuals is highly complex (Ueda and Bell, 2021), and furthermore that we should not expect modern and ancient samples to reflect local $\delta^{18}O_{precip}$ values to the same degree.

Although previous studies have suggested that breastfeeding or physiological changes may lead to isotopic enrichment of bone mineral $\delta^{18}O$ values (reviewed in Pederzani and Britton, 2019), neither the M1s in the current study (Fig. 2), nor a similar number of wild primate M1s also measured with the SHRIMP-SI (Green et al., 2022) show evidence of isotopic enrichment during the first year, when milk would constitute the great majority of ingested liquids. Moreover, a recent study of serially-forming wild orangutan molars did not find noteworthy differences between M1s and M2s/M3s in the same four individuals (Smith et al., 2023). It appears that M1 enamel returns values that are as informative of seasonal $\delta^{18}O$ amplitudes as later forming teeth.

4.2. Isotopic inference of childhood residence

$^{87}Sr/^{86}Sr$ ratios of the archaeological teeth were used to determine whether any individuals may have been non-local to the site where they were buried. The $^{87}Sr/^{86}Sr$ ratios of archaeological humans from Con Co Ngua (Vietnam) measured here lie in the same range as the ratios of archaeological humans (n = 40) previously measured from the same site (0.7095 ± 0.0002) (Huffer et al., 2022). The narrow range of values reflects the well mixed composition of the surrounding alluvial landscape composed of sediment originating from substrates with lower ratios (limestones and Permian to Early Triassic marine sediment; ~0.7070–0.7085, Huffer et al., 2022) and higher ratios (igneous outcrops and granites, dacites and rhyolites, ~0.7080–0.720). Thus, the results suggest that the diets of the humans were composed of food items sourced from the surrounding alluvial catchment as well as from marine resources.

The site of Napa (Philippines) sits on Pliocene-Pleistocene Limestones, and the Bondoc Peninsula consists almost entirely of sedimentary rocks (Pratt, 1914; Aurelio et al., 2013). Due to its coastal location and underlying geology, the immediate baseline is expected to be ~0.7092, but the proximity of volcanic activity may lower the regional $^{87}Sr/^{86}Sr$ baseline. $^{87}Sr/^{86}Sr$ ratios of rocks, lava and volcanic dust measured from locations close to Napa, Philippines record ratios between 0.7037 and 0.7048 (Mukasa et al., 1994; Castillo and Newhall, 2004; Maussen et al., 2018); all lower compared to the $^{87}Sr/^{86}Sr$ ratios of the archaeological humans measured in this study. This suggests that the human diets were composed of a mixture of food sources originating from coastal locations influenced by strontium sea-spray as well as food sources growing in closer proximity to volcanic geology.

On the island of Flores, Indonesia, the geology is composed of Neogene and intermediate basic volcanic rocks (O'Sullivan et al., 2001). Thus, the less radiogenic values of the archaeological humans measured from Pain Haka are consistent with consumption of food items from the immediate landscape. However, we also cannot exclude the possibility that they originated from distant locations that have the same underlying geology and $^{87}Sr/^{86}Sr$ ratio composition.

There is a general lack of evidence to suggest that any of the individuals in this study record non-local climate and rainfall patterns. Most samples at each site form a tight cluster, likely reflecting diets obtained from the local landscape. Those that fall outside the site-specific clusters (M80 in CCN and PH47B at PH) may possibly be non-local. However, if they are non-local, they do not have disparate $\delta^{18}O$ sequences compared to the remaining individuals at each site, which may be the result of originating from a similar latitude or place with similar regional weather patterns.

4.3. Implications for future isotopic studies

It is important to note that seasonal variability in $\delta^{18}O_{precip}$ values does not always correlate to indices of relative seasonality of rainfall (Schwartz et al., 2020; Walsh and Lawler, 1981; Feng et al., 2013). Oxygen isotope fractionation in rainfall is affected by factors including air temperature and source of airmasses bringing in rainfall with varying stable oxygen isotope compositions (Dansgaard, 1964) that do not necessarily impact on the timing, duration, and intensity of rainfall events. Using the R script provided in Schwartz et al. (2020) and the GNIP data used in this study, the seasonality indices for the study locations are as follows:

1) Feng et al. (2013) index: 0.133 (Indonesia), 0.135 (Vietnam), 0.240 (Philippines)
2) Walsh and Lawler (1981) index: 0.591 (Indonesia), 0.770 (Vietnam), 0.814 (Philippines)

These indices suggest that the differences between the summer amounts of rainfall and the winter amounts of rainfall are highest in the Philippines and lowest in Indonesia, consistent with the pattern shown in Fig. 3. However, Fig. 3 also shows that the seasonal differences in rainfall amounts do not map directly onto the amplitudes of seasonal $\delta^{18}O_{precip}$ variability. This underscores the need to acknowledge that while the seasonal differences in $\delta^{18}O_{precip}$ provide useful information about the factors impacting the $\delta^{18}O$ composition of rainfall (such as temperature and air mass composition), they cannot be used to provide a full picture of the relative seasonality of rainfall in a given location. As a result, the variability in $\delta^{18}O_{enamel}$ values is best employed in paleoclimate research to assess possible shifts in rainfall patterns in one location (e.g., through an assessment of changing amplitudes of seasonal $\delta^{18}O_{precip}$ variation through time) rather than to compare the degrees of seasonality between different regions.

Furthermore, the measured $\delta^{18}O_{enamel}$ values can only be used to infer aspects of past rainfall seasonality, and not as a technique for determining with certainty *where* any given individuals lived during tooth formation (also see Pederzani and Britton, 2019; Ueda and Bell, 2021; Pryor et al., 2014). A mean intra-tooth value of 16 ‰ recorded from a human tooth would be consistent with residence at any of the 3 studied locations; it is only when full annual seasonality amplitudes are considered for larger numbers of samples that a non-local origin of an individual might be more reliably inferred. The SHRIMP method provides more accurate estimates of seasonal variability in $\delta^{18}O$ of water intake than lower-resolution methods, which—by sampling across larger areas of sequentially forming enamel—produce more averaged $\delta^{18}O$ values of water intake (Balasse, 2003).

In conclusion, fine-scale $\delta^{18}O_{enamel}$ sequences measured on archaeological teeth can provide useful information for identifying climate variation experienced by past individuals. We caution that these results cannot be used to determine exact geographic origins of the studied individuals (see also Pryor et al. (2014). Future studies may focus on assessing chronological changes in the seasonal variability of $\delta^{18}O_{enamel}$ from individuals recovered at the same site, while tempering conclusions about the degrees of relative rainfall seasonality across different environments. In regions like Southeast Asia, where $\delta^{18}O$ values of precipitation are predominantly driven by amount of precipitation and shifting water sources (Wolf et al., 2020; Araguás-Araguás et al., 1998; Modon Valappil et al., 2022), changes to seasonal variation in $\delta^{18}O$ values of past precipitation can be used to assess shifts in the behaviors of tropical monsoons. This can provide a more nuanced climatic background for investigating aspects of human adaptation to these landscapes.

Ethics declaration

Modern teeth were not extracted for the purposes of this study, but

shared with the researchers after their clinical removal. Consent was obtained from the individuals and/or their legal guardians.

Authors contributions

Rebecca Kinaston: Formal analysis, Methodology, Resources, Writing – review & editing. Hannah F. James: Formal analysis, Investigation, Writing – review & editing. Siân Halcrow: Conceptualization, Data curation, Writing – review & editing. Ian S. Williams: Formal analysis, Methodology, Software, Writing – original draft, Writing – review & editing. Hallie Buckley: Conceptualization, Data curation, Resources, Writing – review & editing. Hiep Hoang Trinh: Data curation, Resources. Janaína N. Ávila: Formal analysis, Methodology, Writing – original draft, Writing – review & editing. Daniel R. Green: Conceptualization, Formal analysis, Methodology, Software, Writing – original draft, Writing – review & editing. Tanya M. Smith: Conceptualization, Data curation, Formal analysis, Methodology, Project administration, Writing – original draft, Writing – review & editing. Jean Christophe Galipaud: Data curation, Resources, Writing – review & editing. Victor Paz: Data curation, Resources. Marc Oxenham: Conceptualization, Formal analysis, Funding acquisition, Writing – review & editing. Christophe Snoeck: Formal analysis, Investigation, Methodology, Resources, Writing – review & editing. Petra Vaiglova: Formal analysis, Writing – original draft, Writing – review & editing. Truman Simanjuknak: Data curation, Resources

Declaration of competing interest

The authors declare that they have no known competing financial interests or personal relationships that could have appeared to influence the work reported in this paper.

Acknowledgements

Technical assistance was provided by Kamil Sokolowski and Brian Tse at the Preclinical Imaging Core Facility at the Translational Research Institute, funding support for which came from Therapeutic Innovation Australia, under the National Collaborative Research Infrastructure Strategy. Histological preparation and SHRIMP analyses were funded by the Australian Academy of Sciences Regional Collaborations Program; Project 'Tracing Ancient Environments During the Peopling of Southeast Asia' (BCC 2017/2305974; Co-PIS: TM Smith, IS Williams, HR Buckley, DR Green) and the Australian Research Council (Future Fellowship FT200100390, PI: TM Smith). The excavation of the Pain Haka site was funded by a grant from the Research Institute for Development, UMR Paloc, and by additional funding from the French Embassy in Indonesia and a University of Otago Research Grant. Regarding the Napa material we thank Mr Ermilando Napa; Captain Leopoldo Quindoza of Barangay Tuhian and the Barangay council; the Sitio Buhangin community; and Jeremy Barns and Angel Bautista of the National Museum of the Philippines. With respect to the Con Co Ngua material grant sponsors included the Australian Research Council DP110101097, FT120100299, FT100100527, and Japan Society for the Promotion of Science 16H02527. Two living tooth donors and their families are also acknowledged with gratitude for their contributions.

Appendix A. Supplementary data

Supplementary data to this article can be found online at https://doi.org/10.1016/j.jas.2023.105922.

References

Araguás-Araguás, L., Froehlich, K., Rozanski, K., 1998. Stable isotope composition of precipitation over southeast Asia. J. Geophys. Res. Atmos. 103, 28721–28742.
Aurelio, M.A., et al., 2013. Structural evolution of bondoc–burias area (South luzon, Philippines) from seismic data. J. Asian Earth Sci. 65, 75–85.
Bagtasa, G., 2017. Contribution of tropical cyclones to rainfall in the Philippines. J. Clim. 30, 3621–3633.
Balasse, M., 2003. Potential biases in sampling design and interpretation of intra-tooth isotope analysis. Int. J. Osteoarchaeol. 13, 3–10.
Belgaman, H.A., et al., 2017. Characteristics of seasonal precipitation isotope variability in Indonesia. Hydrological Research Letters 11, 92–98.
Bellwood, P., 2005. First Farmers: the Origins of Agricultural Societies. Blackwell Publishing.
Bellwood, P., 2011. Holocene population history in the pacific region as a model for worldwide food producer dispersals. Curr. Anthropol. 52, S363–S378.
Bentley, R.A., 2006. Strontium isotopes from the Earth to the archaeological skeleton: a review. J. Archaeol. Method Theor 13, 135–187.
Blumenthal, S.A., et al., 2014. Stable isotope time-series in mammalian teeth: in situ δ18O from the innermost enamel layer. Geochem. Cosmochim. Acta 124, 223–236.
Bowen, G.J., 2010. Isoscapes: spatial pattern in isotopic biogeochemistry. Annu. Rev. Earth Planet Sci. 38, 161–187.
Brockman, D.K., van Schaik, C.P., 2005. Seasonality in Primates: Studies of Living and Extinct Human and Non-human Primates. Cambridge University Press.
Bronson, F.H., 1995. Seasonal variation in human reproduction: environmental factors. Q. Rev. Biol. 70, 141–164.
Bryant, D.J., Froelich, P.N., 1995. A model of oxygen isotope fractionation in body water of large mammals. Geochem. Cosmochim. Acta 59, 4523–4537.
Cai, Y., et al., 2015. Variability of stalagmite-inferred Indian monsoon precipitation over the past 252,000 y. Proc. Natl. Acad. Sci. USA 112, 2954–2959.
Castillo, P.R., Newhall, C.G., 2004. Geochemical constraints on possible subduction components in lavas of mayon and taal volcanoes, southern luzon, Philippines. J. Petrol. 45, 1089–1108.
Cheng, H., et al., 2016. The Asian monsoon over the past 640,000 years and ice age terminations. Nature 534, 640–646.
Dansgaard, W., 1964. Stable isotopes in precipitation. Tellus 16, 436–468.
Deniel, C., Pin, C., 2001. Single-stage method for the simultaneous isolation of lead and strontium from silicate samples for isotopic measurements. Anal. Chim. Acta 426, 95–103.
d'Angela, D., Longinelli, A., 1990. Oxygen isotopes in living mammal's bone phosphate: further results. Chem. Geol. Isot. Geosci. 86, 75–82.
Epstein, S., Sharp, R.P., 1959. Oxygen isotope studies. Trans. Am. Geophys. Union 40, 81–88.
Feng, X., Porporato, A., Rodriguez-Iturbe, I., 2013. Changes in rainfall seasonality in the tropics. Nat. Clim. Change 3, 811–815.
Frew, R., Van Hale, R., Moore, T., Darling, M., 2011. A stable isotope rainfall map for the protection of New Zealand's biological and environmental resources. Report to New Zealand Ministry for Primary Industries. Biosecurity.
Gat, J.R., 1996. Oxygen and hydrogen isotopes in the hydrologic cycle. Annu. Rev. Earth Planet Sci. 24, 225–262.
Global, I.A.E.A., 2022. Network of Isotopes in Precipitation.
Green, D.R., et al., 2022. Fine-scaled climate variation in equatorial Africa revealed by modern and fossil primate teeth. Proc. Natl. Acad. Sci. USA 119, e2123366119.
Griffiths, M.L., et al., 2009. Increasing Australian–Indonesian monsoon rainfall linked to early Holocene sea-level rise. Nat. Geosci. 2, 636–639.
Haberle, S.G., 1998. Late quaternary vegetation change in the tari basin, Papua New Guinea. Palaeogeogr. Palaeoclimatol. Palaeoecol. 137, 1–24.
Hamilton, R., Stevenson, J., Li, B., Bijaksana, S., 2019. A 16,000-year record of climate, vegetation and fire from Wallacean lowland tropical forests. Quat. Sci. Rev. 224, 105929.
Higham, C.F.W., 2021. The later prehistory of Southeast Asia and southern China: the impact of exchange, farming and metallurgy. Asian Archaeology 4, 63–93.
Hollins, S.E., Hughes, C.E., Crawford, J., Cendón, D.I., Meredith, K.T., 2018. Rainfall isotope variations over the Australian continent – implications for hydrology and isoscape applications. Sci. Total Environ. 645, 630–645.
Huffer, D., Oxenham, M., 2016. Investigating activity and mobility patterns during the mid-Holocene in northern Vietnam. In: Oxenham, M., Buckley, H.R. (Eds.), The Routledge Handbook of Bioarchaeology in Southeast Asia and the Pacific Islands. Routledge.
Huffer, D., Bentley, A., Oxenham, M., 2022. Community and kinship during the transition to agriculture in Northern Vietnam. In: Higham, C., Kim, N.C. (Eds.), The Oxford Handbook of Early Southeast Asia. Oxford University Press.
Ickert, R.B., et al., 2008. Determining high precision, in situ, oxygen isotope ratios with a SHRIMP II: analyses of MPI-DING silicate-glass reference materials and zircon from contrasting granites. Chem. Geol. 257, 114–128.
King, C.L., et al., 2013. Moving peoples, changing diets: isotopic differences highlight migration and subsistence changes in the Upper Mun River Valley, Thailand. J. Archaeol. Sci. 40, 1681–1688.
Kohn, M.J., 1996. Predicting animal δ18O: accounting for diet and physiological adaptation. Geochem. Cosmochim. Acta 60, 4811–4829.
Konecky, B., Russell, J., Bijaksana, S., 2016. Glacial aridity in central Indonesia coeval with intensified monsoon circulation. Earth Planet Sci. Lett. 437, 15–24.
Kramer, R.T., et al., 2021. Strontium (87Sr/86Sr) isotope analysis of the Namu skeletal assemblage: a study of past human migration on Taumako, a Polynesian Outlier in the eastern Solomon Islands. Am. J. Phys. Anthropol. 174, 479–499.
Kubat, J., et al., 2023. Dietary strategies of Pleistocene Pongo sp. and Homo erectus on java (Indonesia). Nat Ecol Evol 7, 279–289.
Lewis, S.C., et al., 2011. High-resolution stalagmite reconstructions of Australian–Indonesian monsoon rainfall variability during Heinrich stadial 3 and Greenland interstadial 4. Earth Planet Sci. Lett. 303, 133–142.
Lloyd-Smith, L., Krigbaum, J., Valentine, B., 2016. Social affiliation, settlement pattern histories and subsistence change in Neolithic Borneo. In: Oxenham, M., Buckley, H.

R. (Eds.), The Routledge Handbook of Bioarchaeology in Southeast Asia and the Pacific Islands. Routledge.
Longin, R., 1971. New method of collagen extraction for radiocarbon dating. Nature 230, 241–242.
Longinelli, A., 1984. Oxygen isotopes in mammal bone phosphate: a new tool for paleohydrological and paleoclimatological research? Geochem. Cosmochim. Acta 48, 385–390.
Longinelli, A., Peretti Padalino, A., 1983. Oxygen isotopic composition of mammal bones as a possible tool for palaeoclimatic studies. First results. Palaeoclimates and palaeowaters: A Collection of Environmental Isotope Studies 105–112.
Marwick, B., Gagan, M.K., 2011. Late Pleistocene monsoon variability in northwest Thailand: an oxygen isotope sequence from the bivalve Margaritanopsis laosensis excavated in Mae Hong Son province. Quat. Sci. Rev. 30, 3088–3098.
Maussen, K., et al., 2018. Geochemical characterisation of Taal volcano-hydrothermal system and temporal evolution during continued phases of unrest (1991–2017). J. Volcanol. Geoth. Res. 352, 38–54.
McArthur, J.M., Howarth, R.J., Bailey, T.R., 2001. Strontium isotope stratigraphy: LOWESS version 3: best fit to the marine Sr-isotope curve for 0–509 ma and accompanying look-up table for deriving numerical age. J. Geol. 109, 155–170.
McDermott, F., et al., 1999. Holocene climate variability in Europe: evidence from δ18O, textural and extension-rate variations in three speleothems. Quat. Sci. Rev. 18, 1021–1038.
Modon Valappil, N.K., Mohan Viswanathan, P., Hamza, V., Sabarathinam, C., 2022. Isoscapes to address the regional precipitation trends in the equatorial region of Southeast Asia. Phys. Chem. Earth, Parts A/B/C 127, 103159.
Mukasa, S.B., Flower, M.F.J., Miklius, A., 1994. The Nd-, Sr- and Pb-isotopic character of lavas from Taal, Laguna de Bay and Arayat volcanoes, southwestern Luzon, Philippines: implications for arc magma petrogenesis. Tectonophysics 235, 205–221.
Oxenham, M., Buckley, H.R., 2016. The population history of mainland and island Southeast Asia. In: Oxenham, M., Buckley, H.R. (Eds.), The Routledge Handbook of Bioarchaeology in Southeast Asia and the Pacific Islands. Routledge.
Oxenham, M.F., et al., 2018. Between foraging and farming: strategic responses to the Holocene thermal maximum in Southeast Asia. Antiquity 92, 940–957.
O'Sullivan, P.B., et al., 2001. Archaeological implications of the geology and chronology of the Soa basin, Flores, Indonesia. Geol. 29, 607.
Park, J., et al., 2019. Abrupt Holocene climate shifts in coastal East Asia, including the 8.2 ka, 4.2 ka, and 2.8 ka BP events, and societal responses on the Korean peninsula. Sci. Rep. 9, 10806.
Pawlik, A.F., 2021. Technology, adaptation, and mobility in maritime environments in the Philippines from the Late Pleistocene to Early/Mid-Holocene. Quat. Int. 596, 109–123.
Paz, V., et al., 2018. The Catanauan Archaeological Project: Report on the 10th Field Season.
Pederzani, S., Britton, K., 2019. Oxygen isotopes in bioarchaeology: principles and applications, challenges and opportunities. Earth Sci. Rev. 188, 77–107.
Pellegrini, M., Snoeck, C., 2016. Comparing bioapatite carbonate pre-treatments for isotopic measurements: Part 2 — impact on carbon and oxygen isotope compositions. Chem. Geol. 420, 88–96.
Poussart, P.F., Evans, M.N., Schrag, D.P., 2004. Resolving seasonality in tropical trees: multi-decade, high-resolution oxygen and carbon isotope records from Indonesia and Thailand. Earth Planet Sci. Lett. 218, 301–316.
Pratt, W.E., 1914. The Geology and Petroleum Resources of Bondoc Peninsula, Tayabas Province, Philippines. University of Kansas.
Pryor, A.J.E., Stevens, R.E., O'Connell, T.C., Lister, J.R., 2014. Quantification and propagation of errors when converting vertebrate biomineral oxygen isotope data to temperature for palaeoclimate reconstruction. Palaeogeogr. Palaeoclimatol. Palaeoecol. 412, 99–107.
Reepmeyer, C., et al., 2011. Obsidian sources and distribution systems in Island Southeast Asia: new results and implications from geochemical research using LA-ICPMS. J. Archaeol. Sci. 38, 2995–3005.
Rigo, M., Trotter, J.A., Preto, N., Williams, I.S., 2012. Oxygen isotopic evidence for Late Triassic monsoonal upwelling in the northwestern Tethys. Geology 40, 515–518.
Schwartz, N.B., Lintner, B.R., Feng, X., Powers, J.S., 2020. Beyond MAP: a guide to dimensions of rainfall variability for tropical ecology. Biotropica 52, 1319–1332.
Semah, A.-M., Semah, F., Moudrikah, R., Frohlich, F., Djubiantono, T., 2004. A late Pleistocene and Holocene sedimentary record in central java and its palaeoclimatic significance. Mod. Quat. Res. Southeast Asia 18, 63–88.
Sharp, Z., 2017. Principles of Stable Isotope Geochemistry. Pearson.
Smith, T.M., et al., 2018. Wintertime stress, nursing, and lead exposure in Neanderthal children. Sci. Adv. 4, 1–9.
Smith, T.M., et al., 2023. Oxygen isotopes in orangutan teeth reveal recent and ancient climate variation. Elife 12.
Stephens, M., Mattey, D., Gilbertson, D.D., Murray-Wallace, C.V., 2008. Shell-gathering from mangroves and the seasonality of the Southeast Asian Monsoon using high-resolution stable isotopic analysis of the tropical estuarine bivalve (Geloina erosa) from the Great Cave of Niah, Sarawak: methods and reconnaissance of molluscs of early Holocene and modern times. J. Archaeol. Sci. 35, 2686–2697.
The Routledge Handbook of Bioarchaeology in Southeast Asia and the Pacific Islands, 2016. Routledge.
Ueda, M., Bell, L.S., 2021. Assessing the predictability of existing water-to-enamel geolocation models against known human teeth. Sci. Rep. 11, 15645.
Vaiglova, P., Lazar, N.A., Stroud, E.A., Loftus, E., Makarewicz, C.A., 2022. Best practices for selecting samples, analyzing data, and publishing results in isotope archaeology. Quat. Int. https://doi.org/10.1016/j.quaint.2022.02.027.
Vallée, F., Luciani, A., Cox, M.P., 2016. Reconstructing demography and social behavior during the neolithic expansion from genomic diversity across island Southeast Asia. Genetics 204, 1495–1506.
van der Kaars, S., Wang, X., Kershaw, P., Guichard, F., Setiabudi, D.A., 2000. A Late Quaternary palaeoecological record from the Banda Sea, Indonesia: patterns of vegetation, climate and biomass burning in Indonesia and northern Australia. Palaeogeogr. Palaeoclimatol. Palaeoecol. 155, 135–153.
Vlok, M., Paz, V., Crozier, R., Oxenham, M., 2017. A new application of the bioarchaeology of care approach: a case study from the Metal Period, the Philippines. Int. J. Osteoarchaeol. 27, 662–671.
Walsh, R.P.D., Lawler, D.M., 1981. Rainfall seasonality: description, spatial patterns and change through time. Weather 36, 201–208.
Wang, Y., et al., 2008. Millennial- and orbital-scale changes in the East Asian monsoon over the past 224,000 years. Nature 451, 1090–1093.
Wang, X., et al., 2018. Precession-paced thermocline water temperature changes in response to upwelling conditions off southern Sumatra over the past 300,000 years. Quat. Sci. Rev. 192, 123–134.
Weis, D., et al., 2006. High-precision isotopic characterization of USGS reference materials by TIMS and MC-ICP-MS. G-cubed 7, 1–30.
Wicaksono, S.A., Russell, J.M., Bijaksana, S., 2015. Compound-specific carbon isotope records of vegetation and hydrologic change in central Sulawesi, Indonesia, since 53,000 yr BP. Palaeogeogr. Palaeoclimatol. Palaeoecol. 430, 47–56.
Wicaksono, S.A., Russell, J.M., Holbourn, A., Kuhnt, W., 2017. Hydrological and vegetation shifts in the wallacean region of central Indonesia since the last glacial maximum. Quat. Sci. Rev. 157, 152–163.
Wolf, A., Roberts, W.H.G., Ersek, V., Johnson, K.R., Griffiths, M.L., 2020. Rainwater isotopes in central Vietnam controlled by two oceanic moisture sources and rainout effects. Sci. Rep. 10, 16482.
Wurster, C.M., et al., 2010. Forest contraction in north equatorial Southeast Asia during the last glacial period. Proc. Natl. Acad. Sci. USA 107, 15508–15511.
Wurster, C.M., et al., 2017. Stable isotope composition of cave guano from eastern Borneo reveals tropical environments over the past 15,000 cal yr BP. Palaeogeogr. Palaeoclimatol. Palaeoecol. 473, 73–81.
Yang, H., Johnson, K.R., Griffiths, M.L., Yoshimura, K., 2016. Interannual controls on oxygen isotope variability in Asian monsoon precipitation and implications for paleoclimate reconstructions. J. Geophys. Res. Atmos. 121, 8410–8428.
Yang, J., Dudley, B.D., Montgomery, K., Hodgetts, W., 2020. Characterizing spatial and temporal variation in 18O and 2H content of New Zealand river water for better understanding of hydrologic processes. Hydrol. Process. 34, 5474–5488.
Zhao, L., et al., 2017. Holocene vegetation dynamics in response to climate change and human activities derived from pollen and charcoal records from southeastern China. Palaeogeogr. Palaeoclimatol. Palaeoecol. 485, 644–660.